Accurate binding of sodium and calcium to phospholipid bilayers by effective inclusion of electronic polarization

Josef Melcr and Hector Martinez-Seara Monne
Institute of Organic Chemistry and Biochemistry, Academy of Sciences of the Czech Republic, Prague 6, Czech Republic

Jiří Kolafa
Department of Physical Chemistry, Institute of Chemical Technology, Prague 6, Czech Republic

Pavel Jungwirth
Institute of Organic Chemistry and Biochemistry, Academy of Sciences of the Czech Republic, Prague 6, Czech Republic and Department of Physics, Tampere University of Technology, P.O. Box 692, FI-33101 Tampere, Finland

O. H. Samuli Ollila*
Institute of Organic Chemistry and Biochemistry, Academy of Sciences of the Czech Republic, Prague 6, Czech Republic and Institute of Biotechnology, University of Helsinki
(Dated: November 4, 2017)

The binding affinities and stoichimetries of Na^+ and Ca^{2+} ions to phospholipid bilayers have not been consistently determined with different experimental and theoretical methods despite their significance and biological relevance in cellular membranes. The ion binding details could be resolved with classical molecular dynamics (MD) simulations, however, the accuracy of the available lipid models has not been sufficient. In this work we show that the binding details of Na^+ and Ca^{2+} ions to 1-Palmitoyl-2-oleoylphosphatidylcholine (POPC) bilayer can be accurately described with a MD simulation model having implicitly included electronic polarization. This is demonstrated by applying the electronic continuum correction (ECC) to a state of the art lipid model for MD simulations of POPC lipid bilayer. The introduced ECC-lipids model reproduces the experimentally measured structural parameters for the ion-free membrane, the response of lipid headgroup to the bound positive charge, and the binding affinities of Na^+ and Ca^{2+} ions. The imperceptible binding of Na^+ ions to POPC bilayer and interactions of Ca^{2+} mainly with phoshpate oxygens in the ECC-lipids model give support to the early intepretations of the experimental spectroscopic data. On the other hand, Ca^{2+} ions form complexes with 1-3 lipid molecules with almost equal probabilities, suggesting more complicated binding stoichimetry than the ternary complex binding model used to interpret the NMR data. The results in this work pave the way for MD simulations of complex biochemical systems with realistic electrostatic interactions in the vicinity of cellular membranes.

I. INTRODUCTION

Cation interactions with cellular membranes play a key role in several biological processes, such as signal propagation in neurons and vesicle fusion. Since the direct measurements of ion-membrane interactions from biological systems are difficult, lipid bilayers are often used as models systems for cellular membranes. Especially the zwitterionic phosphocholine (PC) lipid bilayers are used to understand the role of ions in complex biological systems [1–3].

Interactions of biological cations, especially Na^+ and Ca^{2+}, with PC bilayers are widely studied in experiments [2–9] and classical MD simulations [10–14]. The details of ion binding are, however, not fully consistent in the literature. Interpretations of non-invansive spectroscopic methods, like nuclear magnetic resonance (NMR), scattering and infrared spectroscopy suggest that Na^+ ions exhibit negligible binding to PC lipid bilayers with submolar concentrations, while Ca^{2+} is observed to specifically bind to phosphate groups of two lipid molecules [4, 5, 7–9, 15–17]. Atomistic resolution molecular dynamics (MD) simulation models, however, predict significantly stronger binding for the cations than NMR experiments [18]. On the other hand, some experiments have also been interpreted to support the predictions from MD simulations [10, 19]. Furthermore, interactions of calcium ions with 3-4 lipids, including also interactions with carbonyl oxygens, have been reported from simulations [10, 11, 13, 14].

Recent work published by the NMRlipids project (`nmrlipids.blogspot.fi`) [18] made an attempt to resolve the apparent controversies. A direct comparison of ion binding affinities to PC bilayers was presented between simulations and experiments by using the electrometer concept, which is based on the experimental NMR data for the lipid headgroup order parameters [20]. Using massive amounts of data collected by Open Collaboration method, it was concluded that the accuracy of the current state of the art lipid models for MD simulations is not sufficient for the detailed interpretation of the cation interactions with PC lipid bilayers [18].

In this work we show that the cation binding behavior in MD simulations of 1-Palmitoyl-2-oleoylphosphatidylcholine (POPC) bilayer can be significantly improved with an implicit inclusion of the electronic polarizability in the polar region of phospholipids, which we apply according to the electronic

*`samuli.ollila@helsinki.fi`

continuum correction (ECC) [21]. Such an approach has been previously shown to improve the behaviour of MD simulations of ions in bulk water [22**?** –24]. We use the the Lipid14 model [25] as a starting point, because it provided one of the best available descriptions of cation binding [18]. The developed ECC-lipids model reproduces the experimentally measurable structural parameters of an ion-free POPC lipid bilayer with the accuracy comparable to the other state of the art lipid models, while surpassing them significantly in the description of the membrane binding affinities to cations and induced structural effects of sodium and calcium ions.

II. METHODS

A. Electronic continuum correction for lipid bilayers

The lack of polarizability in standard MD simulation force fields has been considered an issue since the early days of lipid bilayer simulations. In this work, we circumvent the rather demanding explicit inclusion of electronic polarization effects [26, 27], including the electronic part of polarizability in lipid bilayer simulations implicitly through the electronic continuum correction (ECC) [21]. Technically, it is similar to the phenomenological charge-scaling applied in earlier studies [28, 29]. **1.We should also cite papers where empirical scaling was used ionic liquids DOI: 10.1002/anie.201308760** However, the present concept of ECC is physically well justified and rigorously derived [21, 30–32].

According to ECC, electronic polarizability can be implicitly included in classical MD simulations by placing all particles into a homogeneous dielectric continuum with a dielectric constant ϵ_{el}, which is the electronic part of the dielectric constant of the media [21]. Following the Coulomb's law, such a dielectric continuum can be easily included in a standard MD simulation by the scaling of charges,

$$Q^{ECC} = f_q \cdot Q, \tag{1}$$

with a constant scaling factor $f_q = \epsilon_{el}^{-1/2}$ effectively representing the newly introduced electronic continuum. Given the high frequency dielectric constant as measured in water (corresponding to the square of the refraction index) of $\epsilon_{el} = 1.78$, the scaling factor for aqueous ions is $f_q = 0.75$ [21**?**]. This scaling factor has been successfully used to improve the performance of force field for ions in solution [23**?** , 24], which then agree quantitatively with neutron scattering data [22–24].

While the scaling factor of $f_q = 0.75$ for ions in water improves their description and is physically well justified within the ECC theory [**?**], it is not a priori clear whether the same factor should be used for partial charges in molecules, e.g., lipids in our case. Unlike the total charge of an atom or molecules, atomic partial charges within molecules are not physical observables. There are thus several schemes for the assignment of partial charges for biomolecules [33]. Currently, the most commonly employed scheme is the restrained electrostatic potential (RESP) method [34, 35]. By construction, partial charges currently implemented in force fields may already include to some extend the solvent electronic polarizability effects, i.e., the RESP charges are subsequently modified to fit certain experimental observables **2.This needs a citation - Joe please pick 1-2 papers**. Thus, a consistent application of the ECC scaling factor, f_q, to the molecular partial charges included in the available force fields does not necessarily have to follow the above relation $f_q = \epsilon_{el}^{-1/2}$, but instead it lies between 0.75 i.e., (no electronic polarizability included in the original partial charges) and 1 (i.e., electronic polarizability fully included in the original partial charges). It is important to note that even though the lipid bilayer interface has a large gradient in the total dielectric constant, the electronic part of polarizability can be considered to be constant as the measurements of high frequency dielectric constant gives values around 2 for almost any biologically relevant material [21**?**].

In this work, we employ the ECC to develop a classical MD simulation model for a POPC lipid that accurately describes the binding of sodium and calcium ions to a lipid bilayer. The quality of the simulation model is compared to the experimental NMR data used to measure the ion binding affinity [4, 5, 36], as discussed in detail in Ref. 18. The Lipid14 [25] force field parameters (available in Gromacs format from Ref. 37) were used as a starting point, because they provide one of the most realistic descriptions of the head group order parameter response to ions among the available lipid models (see Figs. 2 and 5 in Ref. 18). Moreover, the Lipid14 model has a relatively realistic glycerol backbone and head group structure compareable to other state of the art lipid models [38].

We applied the ECC correction to the Lipid14 model of POPC as a scaling of partial charges of the head group, glycerol backbone, and carbonyl regions, which are the most polar parts in phospholipids being expected to have the largest contribution to the cation binding. We do not modify the hydrocarbon chain parameters, as they do not come in direct contact with salt ions, and as they are already highly optimized to provide a good description of the hydrophobic part of lipid bilayers [25, 39]. This is in contrasts with the glycerol backbone and the head group regions, which call for improvements in all available lipid models [38].

The values within the above discussed parameter space for the scaling factor, $f_q \in (0.75, 1.0)$, were explored to find the optimal value to reproduce the experimental ion binding affinity. We observed that the scaling of the partial charges reduced the ion binding affinity and the related head group order parameter response in general. We compared the results with different scaling factors to the experimental NMR data [4, 5, 36] finding the optimal value $f_q = 0.8$, which is only slighly higher than the scaling factor for the ions in water, 0.75.

Although the scaling of the partial charges improved the head group order parameter response and ion binding affinity, it also deteriorated some membrane properties; namely the area per lipid decreased below the experimental value. After only scaling the partial charges of the head group, the glycerol backbone and carbonyls with a factor of 0.8, the area per lipid in the simulation drops to approximately 60 Å^2, which is significantly smaller than the experimental value, 64.3 Å^2

[40], as well as the value from the original Lipid14 model, 65.6 ± 0.5 Å^2 [25]. The decrease of the area per lipid is found to arise from a reduced hydration of the lipid head group region as a consequence of the lower polarity after scaling charges. This effect can be compensated by reducing the effective radii of atoms with the scaled charges. This is in practice done by changing the parameters σ in the Lennard-Jones potential in a similar way as was previously done for the ECC-ions in solution [22–24]. After reducing the σ parameters of affected atoms with a scaling factor $f_\sigma = 0.89$, the area per molecule is restored back close to the experimental value (Table I).

B. Electrometer concept

Ion binding in lipid bilayers was compared between experiments and simulations using the lipid head group order parameters and the "electrometer concept" [18, 20], which is based on the experimental observation that the C-H bond order parameters of α and β carbons in a PC lipid head group (Fig. 1) are proportional to the amount of charge bound per lipid [20]. The change of the order parameters measured with varying aqueous ion concentration can be then related to the amount of bound ions.

The concept can be used to compare the ion binding affinity to lipid bilayers between MD simulations and NMR experiments, because the order parameters can be accurately determined from both techniques [18, 39]. The order parameters for all C-H bonds in lipid molecules, including α and β segments in head group, can be accurately measured using ^{2}H NMR or ^{13}C NMR techniques [39]. From MD simulations the order parameters can be calculated using the definition

$$S_{\mathrm{CH}} = \frac{3}{2}\langle \cos^2\theta - 1 \rangle, \tag{2}$$

where θ is the angle between the bond and membrane normal and the average is taken over all sampled configurations [39].

The relation between the amount of the bound charge per lipid, $X^{\pm}$, and the head group order parameter change, ΔS^i_{CH}, is empirically quantified as [20, 41]

$$\Delta S^i_{\mathrm{CH}} = S^i_{\mathrm{CH}}(X^{\pm}) - S^i_{\mathrm{CH}}(0) \approx \frac{4m_i}{3\chi} X^{\pm}, \tag{3}$$

where $S^i_{\mathrm{CH}}(0)$ denote the order parameter in the absence of bound charge, i refers to either α or β carbon, m_i is an empirical constant depending on the valency and position of the bound charge, and the experimental value [42, 43], $\chi \approx 167$ kHz, is used for the quadrupole coupling constant. Atomic absorption spectra and ^{2}H NMR data gave $m_\alpha = -20.5$ kHz and $m_\beta = -10.0$ kHz for the binding of Ca^{2+} to POPC bilayer (in the presence of 100 mM NaCl) [5, 18, 39]. The slopes are negative, because the head group order parameters decrease with a bound positive charge and increase with a bound negative charge [18, 39]. This can be rationalized as a change of the lipid head group dipole tilt towards water phase with the bound positive charge and *vice versa* with the negative charge [20].

The measured order parameter change depends on both the head group response to the bound charge, and the amount of bound charge (i.e. m_i and $X^{\pm}$ in Eq. 3, respectively). The empirical factor m_i has to be well quantified before the electrometer concept can used to analyze the binding affinities. This was done experimentally for a wide range of systems [20, 44]. To calibrate the head group order parameter response to the bound charge in simulations, we use the experimental data for dihexadecyldimethylammoniumbromide mixed within a POPC bilayer [36]. Dihexadecyldimethylammonium

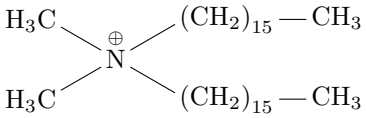

is a cation surfactant having two acyl chains and bearing a unit charge in the hydrophilic end. Thus, it is expected to locate in the bilayer similarly to the phospholipids and the molar ratio then gives directly the amount of bound unit charge per lipid $X^{\pm}$ in these systems [36].

C. Salt concentrations and binding affinity

The concentrations of salts are reported in two different ways in the NMR measurements of head group order parameters [4, 5]. The early work on the NMR electrometer concept reports the salt concentrations in water before solvating the lipids [4]. The later study uses the atomic absorption spectroscopy, and reports the salt concentration in the supernatant after the solvation of lipids [5]. In this work, we focus on POPC for which the latter definition was used [5]. The salt concentration in the aqueous bulk region was calculated from the farthest point from both lipid leaflets in the water phase. Note that in the previous study [18], the ion concentrations were calculated in water before solvating the lipids as in the earlier experiments [4]. Although there are measurable differences between these two definitions of concentrations for $CaCl_2$ systems, they do not affect the qualitative conclusions in this or in the previous work [18].

To quantify the ion binding affinity to a lipid bilayer, we calculate the relative surface excess of ions with respect to water, Γ^w_i [45]. Such a quantity compares the adsorption of ions to the adsorption of water molecules at an interface without the necessity of defining the Gibbs dividing plane between the membrane interior and the water bulk region. In our simulations we assume that the interface locates between the hydrophobic interior of a lipid bilayer and the bulk water region far from the membrane. The bulk concentration of ions and water is zero inside the bilayer. The concentrations in bulk water region can be calculated from the farthest point from both lipid leaflets in the water phase. The region between these boundaries contains all the ions and water molecules in the simulation box. Such a setup provides a simplified relation

for Γ_i^w for simulations of lipid bilayers,

$$\Gamma_i^w = \frac{1}{2A_b}\left(n_i - n_w\frac{C_i}{C_w}\right), \quad (4)$$

where n_w and n_i are the total number of waters and ions in the system; C_w and C_i are their respective bulk concentrations in the aqueous phase; and A_b is the area of the box in the membrane plane. The total area of the interface is twice the area of the membrane, $2A_b$, because bilayers have an interface at both leaflets.

D. Validation of lipid bilayer structure against experiments

The structure of lipid bilayers in simulations without ions were validated against NMR and x-ray scattering experiments by calculating the order parameters for C-H bonds and the scattering form factors. The former validates the structures sampled by the individual lipid molecules in simulations with atomic resolution, while the latter validates the dimensions of the lipid bilayer (thickness and area per molecule) [39].

The order parameters were calculated from simulations for all C-H bonds in lipid molecules from Eq. 2. Form factors were calculated from the equation

$$F(q) = \int_{-D/2}^{D/2} (\rho_{el}(z) - \rho_{el}^s)\cos(zq_z)\mathrm{d}z, \quad (5)$$

where $\rho_{el}(z)$ is the total electron density, ρ_{el}^s is the electron density of the solvent far in the bulk, and z is the distance from the membrane centre along its normal spanning until the water bulk region, $D/2$.

E. Simulation details

1. *Simulations of POPC bilayers with aqueous ions*

Simulations of a POPC bilayer in a pure water or in varying salt concentrations contained 128 POPC molecules and approximately 50 SPC/E water [46] molecules per each lipid in an orthorhombic simulation box with periodic boundary conditions. The chosen water model was used in the previous parametrization of ECC-ions [22, 24**?**], and it has dielectric properties consistent with ECC [21, 32]. Results with other water models are available in SI (OPC [47], OPC3 [48], TIP3P [49], TIP3p-FB and TIP4p-FB [50], and TIP4p/2005 [51]). Sodium, calcium and chloride ions were modeled as ECC-ions with parameters from 22**?** . Simulation with the Lipid14 model used the TIP3p water model [49] and the ion model by Dang et al. [52–54]. Simulation data for the Lipid14 model with Åqvist [55] ions and TIP3P [49] water models reported in [18] were taken directly from [56–59]. MD simulations were performed using the GROMACS [60] simulation package (version 5.1.4). The simulation settings used in this work are summarized in Table IV. Simulation trajectories and parameters are available at [**?**] 3.To be uploaded to Zenodo.

TABLE I: Values of the area per lipid (APL) of POPC bilayers without ions from the Lipid14 simulation ran in this work and from the literature [25], from the ECC-lipids model, and from experiments.

model	APL (Å^2)	Temperature [K]
Lipid14	65.1± 0.6	300
Lipid14 [25]	65.6± 0.5	303
ECC-lipids	63.2± 0.6	300
experiment [40]	64.3	303

2. *Simulations of POPC bilayers with cationic surfactants*

The structure of dihexadecyldimethylammonium was created with an automated topology builder [61]. The AmberTools program [62] was then used to generate the Amber-type force field parameters. The parameters were converted to the Gromacs format with the acpype tool [63]. The partial charges were then manually modified to approximately correspond to their equivalent segments in Lipid14 [25]. The parameters together with the simulation data are available at [64–69]. The surfactants were randomly placed among the lipids to form bilayer structures with mole fractions of 10%, 20%, 30%, 42%, or 50% of surfactant in the POPC bilayer. All systems contained 50 POPC molecules per leaflet, 6340 TIP3P [49] water molecules and 6, 14, 21, 35, or 50 surfactants per leaflet. Note that chloride counter ions were used in simulations, but bromide was used as a counter ion in the experiment [36]. The Lipid14 model was used for POPC. The first 20 ns of the total simulation time of 200 ns was considered as an equlibration time and was omitted from the analysis. A reasonable lipid neighbor exchange occured during the simulations.

The same systems were also simulated with the ECC-lipids model for POPC and SPC/E model for water using the same setup. In these simulations ECC was also applied to the cationic surfactant in the same way as to POPC; all charges were scaled with the same factor as for ECC-lipids, i.e. $f_q = 0.8$, and the same atom types with reduced σ parameters from ECC-lipids were used. 4.Provide the parameteres for ECC-surfactant somewere.

III. RESULTS AND DISCUSSION

A. POPC membrane structure and dynamics

The ECC-lipids and Lipid14 models reproduce the experimental x-ray scattering form factors of a POPC bilayer with a similar accuracy in Fig. 1. The area per lipid values from the Lipid14 model is slightly larger than the experimental value in Table I, while the value from ECC-lipids model is slightly smaller. The values of the area per lipid of the ECC-lipids model show some variation when simulated with different water models in Table III (Supplementary Information), however, all the values are close to the experimentally reported values. In conclusion, the ECC-lipids model reproduces the experimental dimensions of POPC lipid bilayer with the accuracy

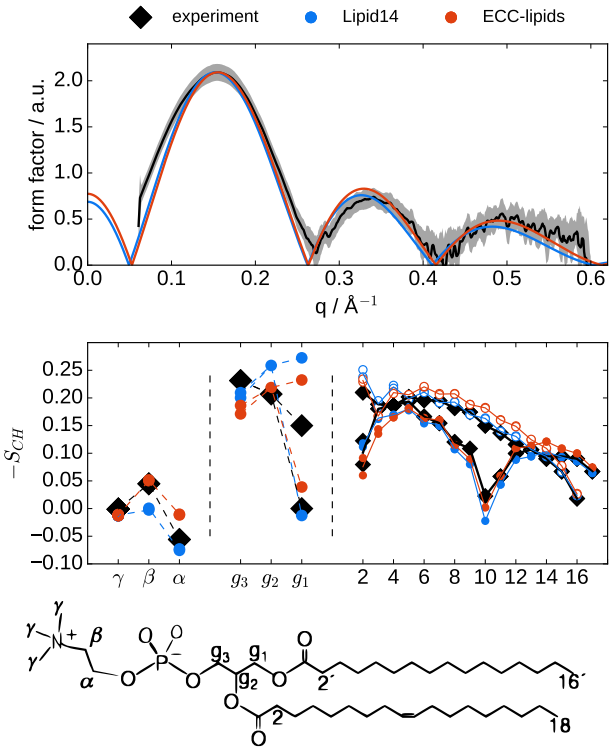

FIG. 1: Top: X-ray scattering form factors from simulations with the Lipid14 [25] and the ECC-lipids models compared with experiments [**?**]. Middle: Order parameters of POPC head group, glycerol backbone and acyl chains from simulations with the Lipid14 [25] and the ECC-lipids models compared with the experimental values from [70]. The size of the markers for the head group order parameters correspond to the error estimate ± 0.02 for experiments [38, 39], while the error estimate for simulations is ± 0.005. The size of the points for acyl chains are decreased by a factor of 3 to improve the clarity of the plot. Bottom: The chemical structure of POPC and the labeling of the carbon segments.

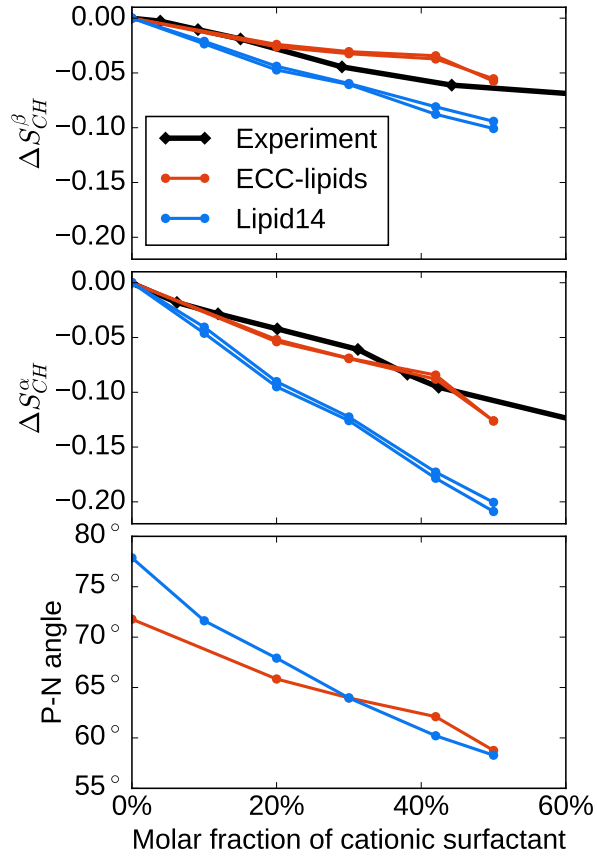

FIG. 2: The changes of headgroup order parameters and P-N vector orientation as a function of cationic surfactant (dihexadecyldimethylammonium) in POPC bilayer from simulations and experiments [36].

comparable to other state of the art lipid models [39].

The acyl chain order parameters of the Lipid14 model [25] and the ECC-lipids model agree with the experimental values with in the error bars in Fig. 1, althought the ECC-lipids model gives slightly larger values for *sn*-1 chain. Notably, the experimentally measured forking and small order parameter values of C_2 segment in *sn*-2 chain are relatively well reproduced by both models. This has been suggested to indicate that the carbonyl of *sn*-2 chain is directed towards the water phase, in contrast to the carbonyl in *sn*-1 chain, which would orient more along the bilayer plane [71–73]. While this may be an important feature for the ion binding details, it is not necessarily reproduced by the available lipid models [39]

The order parameters of α and β carbons in the headgroup are slightly larger in the ECC-lipids model than in the Lipid14 model, which is apparently related to the P-N vector orienting 7° more toward the water phase in the ECC-lipids model, see Fig. 2. With the current data we cannot, however, conclude which one of the models give the more realistic headgroup conformations. The ECC-lipids model gives the β carbon order parameter value closer to experiments, while value for α carbon is better in the Lipid14 model. Despite some deviations from the experimental order parameter values in Fig. 1, the accuracy of the both models in the glycerol backbone region is comparable to the other state of art lipid models available in literature [38].

5.Dynamics check is missing: MSD (Hector/Joe)

B. Calibration of lipid electrometer: Response of POPC head groups to bound charge

Before proceeding to the ion binding affinity, we quantify the response of the headgroup order parameters to the amount of bound charge by using mixtures of monovalent cationic surfactants (dihexadecyldimethylammonium) and POPC [36]. The amount of bound charge per PC in these systems is given by the molar fraction of cationic surfactants, because essentially all surfactants with two hydrophopic acyl chains can be assumed to locate in the lipid bilayers. The experimental data for these systems can be used to validate the sensitivity of lipid headgroup order parameters to the amount of bound charge in simulations.

The changes of the headgroup order parameters with an increasing amount of the cationic surfactant is compared between experiments [36] and simulations in Fig. 2. Approximately linear decrease of the order parameters, as expected from Eq. 3, is observed in simulations and experiments at least for the mole fractions below $\sim$30%. The slope is, however, too steep in the Lipid14 model indicating that the head group order parameters respond too sensitively to the bound positive charge. The slope in the ECC-lipids model is in a very good agreement with experiments for the α segment, while the slope is slightly underestimated for the β segment.

The headgroup P-N vector angle with respect to the membrane normal is also shown in Fig. 2 as a function of the mole fraction of the cationic surfactant. As suggested previously [20], the headgroup orients more towards the water phase with the increasing amount of positive charge in a PC lipid bilayer. The effect is more pronounced in the Lipid14 model, for which the addition of 50% mole fraction of the cationic surfactant leads to the decrease of 20° of the P-N vector angle, while the corresponding change in the ECC-lipids model is 11°. The difference is in line with the smaller order parameter changes and the reduced charge–dipole interactions in the latter model. The lower sensitivity of the P-N vector angle response in the ECC-lipid model can be considered to be more realistic, because the changes of the headgroup order parameters as a function of the bound positive charge are in better agreement with experiments in this model. The results also imply that the validation and improvements of MD simulation models are generally required for the reliable simulation studies of the lipid headgroup responses to ions or other biomolecules, as also concluded previously [38].

C. Binding affinities to POPC membrane validated through lipid electrometer

The changes of the lipid bilayer headgroup order parameter from different simulations and experiments [4, 5] are shown in Figs. 3 and 4 as a function of NaCl and $CaCl_2$ concentrations. These results can be used to compare the ion binding affinities to lipid bilayers between simulations and experiments using the electrometer concept, because the order parameters decrease proportionally to the amount of bound positive charge (Fig. 2 and Ref. 18, 20). The recent comparison of different simulation models to the experimental data revealed that most models significantly overestimate Na^+ ion binding to PC lipid bilayers and that none of the available models correctly reproduces the details of the binding of Ca^{2+} ions [18]. A positive exception in Ref. 18 was the Lipid14 model [25] simulated with Åqvist ions. Such a combination of models reproduced the experimentally measured small order parameter changes with NaCl (Fig. 4) and imperceptible Na^+ binding to PC bilayers [4, 5]. However, the changes of the headgroup order parameters as a function of $CaCl_2$ concentration (Fig. 3) were overestimated by the same combination of force field parameters.

Since significant artefacts are reported in simulations with Åqvist ions is water [74], we also simulated the Lipid14 model

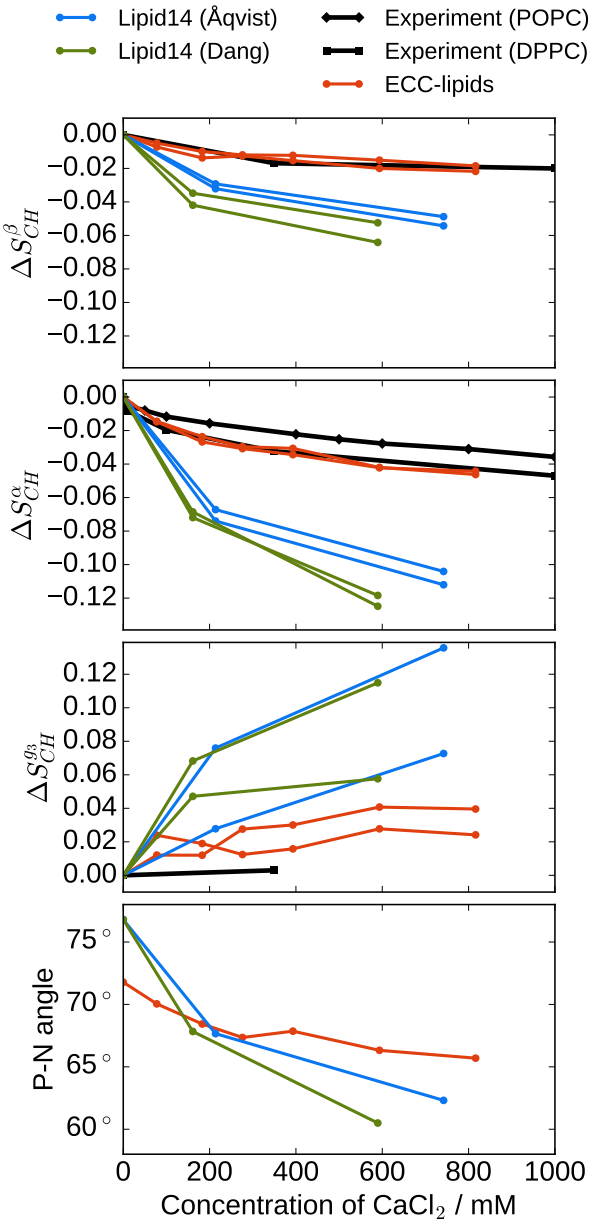

FIG. 3: The changes of the head group order parameters of POPC bilayer as a function of $CaCl_2$ concentrations are shown from simulations with different force fields together with experimental data (DPPC [4] and POPC [5]). Ion concentrations in bulk water are shown in x-axis. Values from simulations are calculated from the of cation number density C_{np} from the region at the simulatin box edge with the constant ion concentration as [ion]=$C_{np}/0.602$. Simulation data with Lipid14 and Åqvist ion parameters are taken directly from Refs. [56–58].

6.Add temperatures for POPC and DPPC experiments

with more realistic ion models by Dang et al. [52–54], and ECC-ions [22**?**]. Instead of an improvement in the binding behaviour, we observed greatly overestimated binding for Ca^{2+} and also for Na^+ with such ions models (Figs. 3 and 4). **8.Add OP-response of Lipid14+ECC-ions plot in SI**. The results are in line

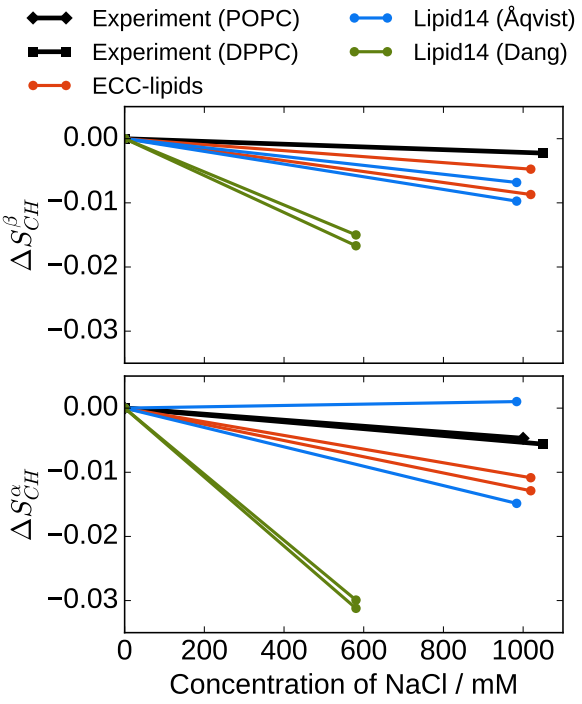

FIG. 4: The changes of the head group order parameters of POPC bilayer as a function of NaCl concentrations from simulations with different force fields together with experimental data for DPPC [4] and POPC [5]. Ion concentrations in x-axis are calculated as in Fig. 3. Simulation data with Lipid14 and Åqvist ion parameters is taken directly from Refs. [56, 59].

7.Add temperatures to the experimental data.

with the previous work [18], suggesting that the improvements in the lipid parameters are required to correctly describe the binding of divalent cations to phospholipid bilayers.

The results from the simulations with the ECC-lipids and the ECC-ion models [22, 24**?**] exhibit an improved behaviour of cation binding to a POPC bilayer in Fig. 3, showing a good agreement with experiments in the changes of the lipid headgroup order parameters as a function of NaCl and $CaCl_2$ concentrations. Since also the headgroup order parameter response the to the bound positive charge the ECC-lipids model was in good agreement with experiments in section III B, we conclude that the model correctly reproduces the binding affinity of Na^+ and Ca^{2+} ions to POPC lipid bilayer.

In addition, the response of the glycerol backbone g_3 order parameter to $CaCl_2$ was signifincantly overestimated in the original Lipid14 model, while the ECC-lipids model gives a greatly improved agreement with exepriments, as seen in Fig. 3. Also the changes of the P-N vector angle are more pronounced for the Lipid14 model, for which the largest tilting toward water phase induced by a 780 mM $CaCl_2$ concentration is approximately 17°, while the corresponding value for ECC-lipids model is 6° (820 mM $CaCl_2$).

Furthermore, the overestimated lipid headgroup order parameter changes of POPC in the Lipid14 model as a function of $CaCl_2$ concentration arise from both, the overestimated

TABLE II: Relative surface excess of calcium with respect to water, and the ratios of the amount of calcium cations bound to phosphate or carbonyl moieties to the amount of such cations bound to both moieties in a POPC bilayer from various simulation models. The $CaCl_2$ concentration of the ions in water before adsorption to the phospholipid bilayer is 350mM in the analyzed systems.

9.Add columns with concentrations of calcium – bulk/molar fraction. 10.Changing symbol P to R or r might reflect better that it is rather a ratio, and not that much a probability.

model	Γ^w_{Ca} (nm^{-2})	$P^{Ca^{2+}}_{PO_4}$	$P^{Ca^{2+}}_{O_{carb.}}$
ECC-lipids	0.06 ± 0.01	99%	25%
Lipid14/Åqvist	0.13 ± 0.01	-	-
Lipid14/Dang	0.23 ± 0.03	-	-
Lipid14/ECC-ions	0.35 ± 0.11	-	-

binding affinity and sensitivity of the headgroup tilt to the bound positive charge. This probably applies also to the other lipid models in a previous study [18], emphasizing the importance of the comparison of the lipid headgroup order parameter response to the bound charge between simulations and experiments as done in section III B.

The ion binding affinity of ECC-lipids model with different water models is compared in SI. In general, the order parameter changes are slightly overestimated with the four-site water models, and with TIP3p. However, the performance of ECC-lipids with any of the water models is better than the original Lipid14 model.

D. Structure and affinity of cation binding to POPC membrane

Binding affinities of Ca^{2+} ions to a POPC bilayer in different simulation models were quantified by calculating the relative surface excess of calcium to water molecules, Γ^w_{Ca}, from Eq. 4. The values of Γ^w_{Ca}, shown in Table II, were calculated from simulations with the same 350 mM concentration of $CaCl_2$ with respect to water, i.e., the concentration before solvating the lipids in experiments. As expected from the changes of the lipid headgroup order parameters in Fig. 3, the relative surface excess for the ECC-lipids model, $\Gamma^w_{Ca} = (0.06 \pm 0.01)\mathrm{nm}^{-2}$, is significantly smaller than for the Lipid14 model with Åqvist ions, $\Gamma^w_{Ca} = (0.13 \pm 0.01)\mathrm{nm}^{-2}$, or with Dang ions, $\Gamma^w_{Ca} = (0.23 \pm 0.03)\mathrm{nm}^{-2}$, or with ECC-ions, $\Gamma^w_{Ca}(0.35 \pm 0.11)\mathrm{nm}^{-2}$, where the large uncertainity arises from a too small simulation box (Fig. 5). Interestingly, the relative surface excess of NaCl at 1 M concentration (ECC-ions [22]) is qualitatively different from $CaCl_2$ having a negative value $\Gamma^w_i = (-0.11 \pm 0.01)\mathrm{nm}^{-2}$ meaning that water molecules are preferred to sodium and chloride ions at the membrane-water interface. This is in contrast to the most of the available lipid force fields, which predict a specific binding of sodium to PC lipid bilayers [18].

The ratio of the amount of calcium cations bound to phosphate or carbonyl moieties to the amount of such cations bound to both moieties in a POPC bilayer from various simulation models were analyzed by counting the contacts within

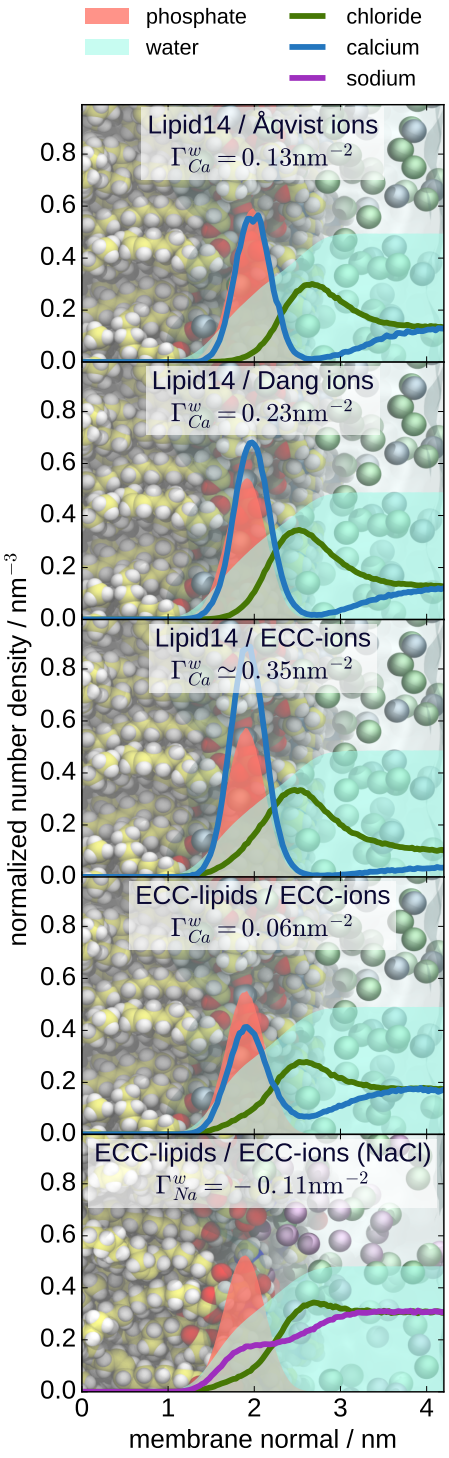

FIG. 5: Number density profiles of Ca^{2+}, Na^+ and Cl^- along membrane normal axis for different force fields. Data for Lipid14 with Åqvist ions are taken directly from Ref. 18. In order to visualize the density profiles with a scale comparable to the profile of Ca^{2+}, densities of Cl^- and Na^+ are divided by 2, and densities of phosphate group resp. water are divided by 5 resp. 200. The molar concentration of ions in water is 350 mM in all systems presented here.

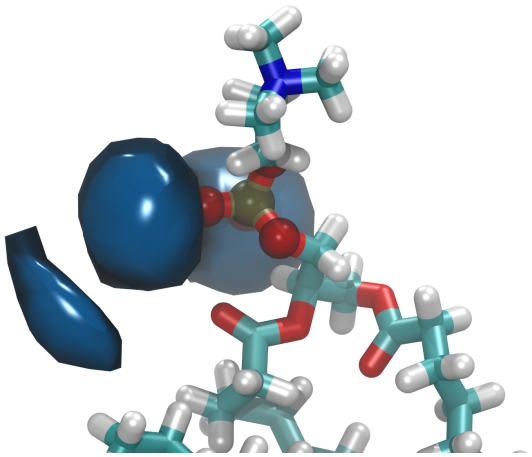

FIG. 6: Isocontours of probability density of Ca^{2+} with respect to the phosphate oxygens of POPC from ECC-lipids simulation. The probability density was evaluated around a single lipid, after its strucutral alignment using only phosphate group.

11.JOE: I'll update this figure with some ensemble of configuration to support binding preference of Ca^{2+} SAMULI: I am not sure if this would be needed anymore.

the distance of $0.3\,\mathrm{nm}$, as done previously in Ref. 14. The results in Table II show that almost all (99%) of the bound Ca^{2+} ions are in contact with the phosphate oxygens, with two thirds (67%) interacting with only phosphate oxygens and the rest, one third (32%), interacting also with the carbonyl oxygens. Thus, the interactions between calcium ions with only carbonyl oxygens are very unlikely (1%), however, a significant amount of the ions interacts with both, phosphate and carbonyl, oxygens moieties. The individual lipids or acyl chains were not distinguished in the analysis, hence, a simultaneous contacts of ions with both oxygen moieties may be inter or intra molecular, and may occur with carbonyls in either of the acyl chains. The most likely interactions between Ca^{2+} ions and phosphate oxygens are visualized with the probability density isocontours in Fig. 6. While the higher concentrations of $CaCl_2$ naturally increased the amount of contacts per lipid, the distribution of contacts between phosphate and carbonyl oxygens was not affected.

Even though Na^+ ions do not specifically bind to a POPC bilayer, they still interact with its oxygen moieties. The results from simulation at $1\,\mathrm{M}$ NaCl concentration show that 55% of Na^+ ions interact with only phosphate oxygens of POPC and 20% with only carbonyl oxygens, and the rest, 25%, is interacting with both.

In conclusion, the results suggest that calcium ions specifically bind to phosphate oxygens occasionally interacting also with carbonyls. This is in good agreement with the previous conclusions from several experimental and theoretical studies [3, 7, 15–17], but suggests lower relative binding affinity to carbonyls than the previous MD simulation studies [10, 11, 13, 14]. Sodium ions also interact most likely with phosphate oxygens of POPC, but in contrast to calcium, the interactions with only carbonyls are also significant. The

physiological relevance of the sodium binding details is, however, uncertain due to its very weak binding affinity.

E. Binding stoichiometry of Na^+ and Ca^{2+} cations to POPC membrane

Simple binding models have been previously used to interpret the same experimental data [5, 75] which are used in this work to validate the simulation models in Fig. 3. The experimental results from the lipid headgroup order parameters and from the atomic absorption spectroscopy were best explained by a ternary complex binding model with a binding stoichiometry of one Ca^{2+} per two POPC lipids [5]. However, also a Langmuir adsorption model (i.e. Ca^{2+}:POPC stoichiometry of 1:1) provided a good fit to the experimental data when only low concentrations of $CaCl_2$ were considered [75]. The results based on these binding models and the measured headgroup order parameter changes are also inluded in the tabulated experimental binding constants [76].

Since the same experimental data is reproduced by the ECC-lipids model, it can be used to give a more versatile interepration of the binding stoichiometry than the previously used simple binding models [5, 75]. To directly evaluate the stoichiometry from simulations we calculated the relative propensities of Ca^{2+}:POPC complexes with various stoichiometries by counting the individual lipid molecules within the distance $0.3\,\mathrm{nm}$ from each Ca^{2+} ion as already used in previous section III D. The results from POPC simulation with 285 mM concetration of $CaCl_2$ in Fig. 7 show the largest propensity (41%) for the ternary complex with the Ca^{2+}:POPC stoichiometry of 1:2, but the probabilities of complexes with the stoichimetries of 1:1 (25%) and 1:3 (34%) are only slightly lower suggesting a more complex binding model than the simple ternary complex model. However, the simulation data can also be viewed from such an angle that one calcium binds roughly to two lipids on average, because the probabilities of the complexes with 1 or 3 lipids are almost equal. This probably explains the success of the ternary complex model fitting well the experimental data. Complexes with more than three lipids per one calcium ion were not observed in simulations with the ECC-lipids model. **12.Samuli: I think that we either have to do the analysis in SI properly, i.e., using the real C_I from simulations or remove the sentence below and the related concent from SI.**
Joe: I think it shows that ternary complex makes a good fit to our simulation data. The fact that we use a different (and more accurate) estimate of C_I and other quantities does not hamper this statement. Ternary complex model also provides a good fit to our simulations with ECC-lipids (see Fig. S8 in SI and its caption for details).

The probabilities of different complexes formed by Na^+ ions and POPC analyzed from the simulation with the ECC-lipids model at 1 M concentration of NaCl are also shown in Fig. 7. In contrast to calcium, the probability is largest (67%) for 1:1 complex, significantly smaller (29%) for 1:2 complexes and very small (4%) for 1:3 of Na^+:POPC complexes.

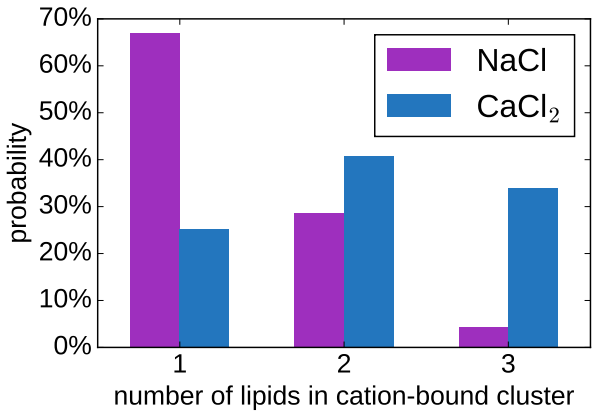

FIG. 7: Relative probabilities of existence of Na^+ or Ca^{2+} complexes with a certain number of POPC lipids. Na^+ complexes were evaluated from the simulation with 1 M concentration; and Ca^{2+} complexes were evaluated from the simulation with 287 mM concentration.

F. Residence times of Na^+ and Ca^{2+} cations in POPC membrane

Equilibration of Ca^{2+} binding to POPC bilayer takes hundreds of nanoseconds in MD simulations with current state of the art force fields, e.g. CHARMM36 and Slipids force fields [14], suggesting that simulations at a temporal scale of several microseconds are required for studies of cation binding in equilibrium. This is in line with the density profiles of Ca^{2+} from simulations in Fig. 5, which all show a region of a very small calcium density around the level of cholines in POPC (i.e. around $2.5\,\mathrm{nm}$) with the exception of ECC-lipids, which exhibits only a relatively shallow local minimum at that level. This suggests that such a smaller barrier for the exchange of calcium ions shall lead to their faster exchange with the solvent. To quantify the exchange of ions between the membrane and solvent in simulations, we calculated residence times of ions bound to the membrane. We again use the definition for ions binding to the membrane as in the above section III D, i.e. ion is bound if it is within 0.3 nm from any oxygen atom belonging to a lipid molecule in a bilayer.

The histograms of residence times of Ca^{2+} in a POPC bilayer at $450\,\mathrm{mM}$ concentration of $CaCl_2$ in water before adsorption to phospholipids from simulations with ECC-lipids and CHARMM36 (taken from previous study [14], simulation data available at Ref. 77) are shown in Fig. S11 in SI. In the CHARMM36 simulation, approximately 20% of the Ca^{2+} residence times are longer than the length of the trajectory ($800\,\mathrm{ns}$). With such a simulation, which is hence relatively short for the employed model, we can merely estimate an upper bound that only less than 60% of the bound residence time is formed by cations interacting with the phospholipid membrane for less then half of the simulation length (400 ns). Even longer residence times are observed in the other simulations with CHARMM36 and Slipids models reported in the previous work [14].

On the other hand, at least an order of magnitude faster ex-

change is observed in the ECC-lipids model, where 90% of the Ca^{2+} residence times to a POPC membrane are shorter than 60 ns, and the longest observed residence time in the ECC-lipids simulation is 141 ns, which is well below the total length of the simulation used for analysis, 200 ns. The exchange of Na^+ ions to a POPC membrane is another order of magnitude faster, giving 90% of the residence times smaller than 1 ns, the longest residence time being 6 ns. Note that the results from both analyzed models are in line with the experimental estimation that the residence time of Ca^{2+} at the individual PC headgroup is shorter than 10 μs [5].

In conclusion, the results from the ECC-lipids model suggest that the exchange of calcium between membrane and solvent occurs within $\sim$ 100 ns timeframe, which is much faster than previously reported [14]. Sodium cations exhibit even a faster exchange. This suggests that simulations with the length of a few hundreds of nanoseconds are sufficient to simulate ion binding to phospholipid bilayers in equilibrium, when realistic force fields are used. This has not been the case with the available lipid force fields, which overestimate the binding strength of the cations [14, 18].

IV. CONCLUSIONS

We used the electrometer concept to show that the binding of Na^+ and Ca^{2+} ions to a POPC lipid bilayer can be accurately described with a classical MD simulation force field, where the electronic polarization is implicitly included using the electronic continuum correction (ECC) [21]. The proposed ECC-lipids model is a significant improvement over other available lipid models, which all overestimate specific cation binding affinities [18]. While the structural details of a POPC lipid bilayer simulated with the ECC-lipids model agree with experiments with an accuracy comparable to the other state of the art lipid models, it also reproduces the experimental lipid head group order parameter responses to a cationic surfactant, NaCl and $CaCl_2$ concentrations.

The good agreement with experiments enables us to interpret NMR experiments in atomistic details using MD simulations. In line with previous interpretations of experimental data [7, 15–17], Ca^{2+} ions interact mainly with phosphate oxygens. However, the stoichiometry of calcium binding is significantly more complicated than in the previous interpretation of the NMR data based on the ternary complex model, where one calcium binds to two POPC molecules [5]. The complexes of one calcium bound to two lipids are the most probable also in the ECC-lipids model, but the complexes of one or three lipids per one calcium were observed to be almost equally likely. While the success of the ternary compex model is understandable based on the simulation results, a simple binding model cannot detect the complex nature of calcium binding to phospholipid bilayers oberved in the simulation.

The accurate description of cation binding to POPC bilayer paves the way for simulations of complex biochemical systems with realistically described electrostatic interactions in the vicinity of cellular membranes. The ECC-lipids model is build by scaling the partial charges and the Van der Waals radii of the headgroup, glycerol backbone and carbonyl atoms of the Lipid14 POPC model [25] with the constant factor of 0.8 and 0.89, respectively. While the Lipid14 model is compatible with the AMBER force field family, the compatibility of the ECC-lipids model may be compromised due to the changes in intermolecular interactions of the scaled atoms. On the other hand, a fully consistent ECC-force field should include the correction also in other than lipid molecules, including water. The work toward this direction and the extension to other lipid molecules and force fields is left for future studies.

This work can be reached as a repository containing all data at `zenodo.org:\dots\dots\dots`.

Acknowledgments

P.J. acknowledges support from the Czech Science Foundation (grant no. 16-01074S) and 600 from the Academy of Finland via the FiDiPro award. **13.Add acknowledgments of Jiri Kolafa. 14.Joe: Thank Metacentrum.**

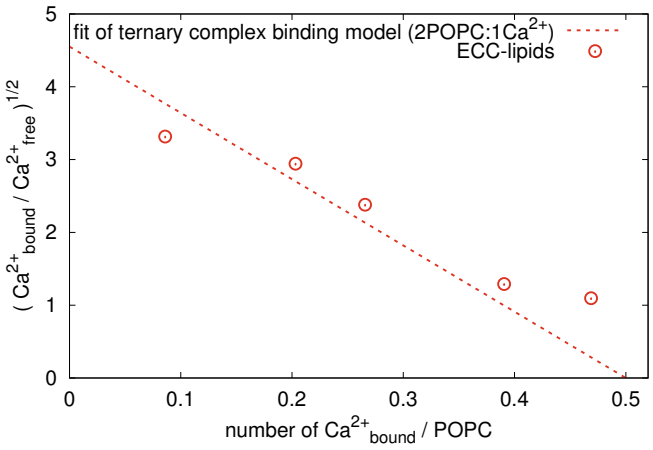

FIG. 8: Ternary complex binding model of Ca^{2+} to a POPC membrane that assumes the stoichiometry of 2 POPC:1 Ca^{2+} (details in reference 5) provides a good fit to experimental measurements [5] and it also provides a good fit to our simulation data. Note that the units in the reference 5 are different from the units presented here, and, hence, the observed slope of the linear relationship is different.

15.This should be either done properly with the correct C_I or removed. Removing might be a better idea at this point. It was found in the original work [5] that a ternary complex binding model (i.e. 2 POPC:1 Ca^{2+}) provides the best fit to experimental measurements of all considered models in that study. In such a model, there is a linear relationship between quantities C_b, mole fraction of bound Ca^{2+} per POPC, and $\sqrt{C_b/C_I}$, where C_I is the concentration of free cations at the plane of ion binding [5]. The concentration C_b was obtained from an extrapolation of linear relation between deuterium NMR measurements and atomic absorption spectroscopy for low concetrations of $CaCl_2$. Such an extrapolation is valid as long as the mode of Ca^{2+} binding remains constant throughout the extrapolation range. The concentration C_I is determined by using the surface potential by using the Boltzmann equation. However, Boltzmann theory yields inaccurate results for divalent cations like Ca^{2+} [78]. An atomistic simulation, on the other hand, provides these quantities directly without severe assumptions. Hence we hypothesise that the discrepancy between the results in the experiment [5] and our simulations likely lays in the fact that the assumptions and relations used for determinig concentrations C_b and C_I in the experiment [5] gradually do not hold for higher concentrations of Ca^{2+}.

SUPPLEMENTARY INFORMATION

TABLE III: Area per lipid (APL) from different models of POPC with no ions

model	APL (Å^2)	Temperature [K]
Lipid14	65.1± 0.6	300
Lipid14 [25]	65.6± 0.5	303
ECC-lipids		
OPC3	62.2± 0.6	300
OPC3	64.2± 0.6	313
SPC/E	65.1± 0.6	313
SPC/E	63.2± 0.6	300
OPC	64.4± 0.6	313
TIP4p/2005	66.8± 0.6	313
TIP3p	66.2± 0.6	313
TIP3p-FB	64.8± 0.6	313
TIP4p-FB	65.6± 0.6	313
experiment	62.7	293
experiment [40]	64.3	303
experiment	67.3	323
experiment	68.1	333

[1] P. Scherer and J. Seelig, The EMBO journal **6** (1987).
[2] J. Seelig, Cell Biol. Int. Rep. **14**, 353 (1990), URL http://dx.doi.org/10.1016/0309-1651(90)91204-H.
[3] G. Cevc, Biochim. Biophys. Acta - Rev. Biomemb. **1031**, 311 (1990).
[4] H. Akutsu and J. Seelig, Biochemistry **20**, 7366 (1981).
[5] C. Altenbach and J. Seelig, Biochemistry **23**, 3913 (1984).
[6] J.-F. Tocanne and J. Teissié, Biochim. Biophys. Acta - Reviews on Biomembranes **1031**, 111 (1990).
[7] H. Binder and O. Zschörnig, Chem. Phys. Lipids **115**, 39 (2002).
[8] G. Pabst, A. Hodzic, J. Strancar, S. Danner, M. Rappolt, and P. Laggner, Biophys. J. **93**, 2688 (2007).
[9] D. Uhrkov, N. Kuerka, J. Teixeira, V. Gordeliy, and P. Balgav, Chemistry and Physics of Lipids **155**, 80 (2008).
[10] R. A. Böckmann, A. Hac, T. Heimburg, and H. Grubmüller, Biophys. J. **85**, 1647 (2003).
[11] R. A. Böckmann and H. Grubmüller, Ang. Chem. Int. Ed. **43**, 1021 (2004).
[12] M. L. Berkowitz and R. Vacha, Acc. Chem. Res. **45**, 74 (2012).
[13] A. Melcrov, S. Pokorna, S. Pullanchery, M. Kohagen, P. Jurkiewicz, M. Hof, P. Jungwirth, P. S. Cremer, and L. Cwiklik, Sci. Reports **6**, 38035 (2016).
[14] M. Javanainen, A. Melcrova, A. Magarkar, P. Jurkiewicz, M. Hof, P. Jungwirth, and H. Martinez-Seara, Chem. Commun. **53**, 5380 (2017), URL http://dx.doi.org/10.1039/C7CC02208E.
[15] H. Hauser, M. C. Phillips, B. Levine, and R. Williams, Nature **261**, 390 (1976).
[16] H. Hauser, W. Guyer, B. Levine, P. Skrabal, and R. Williams, Biochim. Biophys. Acta - Biomembranes **508**, 450 (1978), ISSN 0005-2736, URL http://www.sciencedirect.com/science/article/pii/0005273678900913.
[17] L. Herbette, C. Napolitano, and R. McDaniel, Biophys. J. **46**, 677 (1984).
[18] A. Catte, M. Girych, M. Javanainen, C. Loison, J. Melcr, M. S. Miettinen, L. Monticelli, J. Maatta, V. S. Oganesyan, O. H. S.

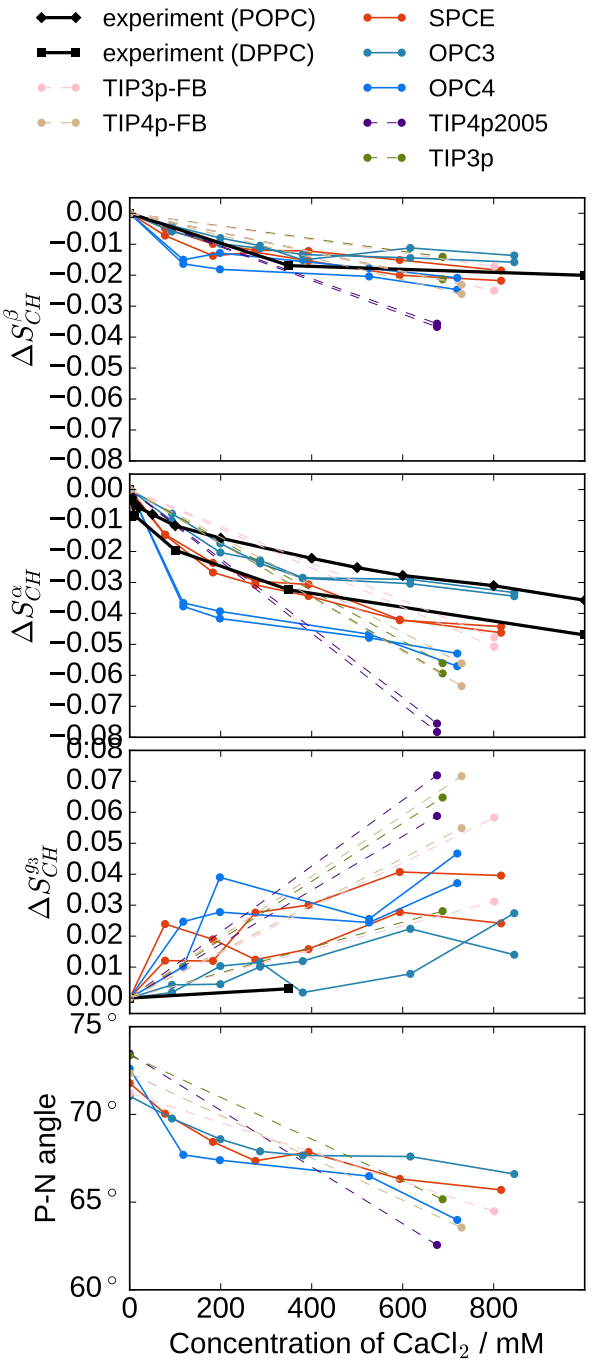

FIG. 9: Changes of head group order parameters of POPC bilayer as a function of $CaCl_2$ concentrations are shown from simulations with different force fields and water models together with experimental data (DPPC [4] and POPC [5]). Ion concentrations in bulk water are shown in x-axis. Values from simulations are calculated from the of cation number density C_{np} from the region at the simulatin box edge with the constant ion concentration as [ion]=$C_{np}/0.602$.

TABLE IV: Simulation parameters

simulation property	parameter
time-step	2 fs
equilibration time	100 ns
total simulation time	300 ns
temperature	313 K
thermostat	v-rescale [79]
barostat	Parrinello-Rahman, semi-isotropic [80]
long-range electrostatics	PME [81]
cut-off scheme	Verlet [82]
Coulomb and VdW cut-off	1.0 nm
constraints	LINCS, only hydrogen atoms [83]
constraints for water	SETTLE [84]

Ollila, et al., Phys. Chem. Chem. Phys. **18** (2016).

[19] R. Vacha, S. W. I. Siu, M. Petrov, R. A. Böckmann, J. Barucha-Kraszewska, P. Jurkiewicz, M. Hof, M. L. Berkowitz, and P. Jungwirth, J. Phys. Chem. A **113**, 7235 (2009).

[20] J. Seelig, P. M. MacDonald, and P. G. Scherer, Biochemistry **26**, 7535 (1987).

[21] I. Leontyev and A. Stuchebrukhov, Phys. Chem. Chem. Phys. **13**, 2613 (2011).

[22] E. Pluhaová, H. E. Fischer, P. E. Mason, and P. Jungwirth, Molecular Physics **112**, 1230 (2014), ISSN 0026-8976, URL `http://www.tandfonline.com/doi/abs/10.1080/00268976.2013.875231`.

[23] M. Kohagen, P. E. Mason, and P. Jungwirth, J. Phys. Chem. B **118**, 7902 (2014).

[24] M. Kohagen, P. E. Mason, and P. Jungwirth, J. Phys. Chem. B **120**, 1454 (2016).

[25] C. J. Dickson, B. D. Madej, . A. Skjevik, R. M. Betz, K. Teigen, I. R. Gould, and R. C. Walker, J. Chem. Theory Comput. **10**, 865 (2014).

[26] T. R. Lucas, B. A. Bauer, and S. Patel, Biochimica et Biophysica Acta (BBA) - Biomembranes **1818**, 318 (2012), membrane protein structure and function.

[27] J. Chowdhary, E. Harder, P. E. M. Lopes, L. Huang, A. D. MacKerell, and B. Roux, J. Phys. Chem. B **117**, 9142 (2013).

[28] B. Jonsson, O. Edholm, and O. Teleman, J. Chem. Phys. **85**, 2259 (1986).

[29] E. Egberts, S.-J. Marrink, and H. J. C. Berendsen, European Biophysics Journal **22**, 423 (1994).

[30] I. V. Leontyev and A. A. Stuchebrukhov, The Journal of chemical physics **130**, 085102 (2009), ISSN 1089-7690, URL `http://scitation.aip.org/content/aip/journal/jcp/130/8/10.1063/1.3060164`.

[31] I. V. Leontyev and A. A. Stuchebrukhov, Journal of Chemical Theory and Computation **6**, 1498 (2010), ISSN 1549-9618, URL `http://dx.doi.org/10.1021/ct9005807`.

[32] I. V. Leontyev and A. A. Stuchebrukhov, Journal of Chemical Physics **141**, 014103 (2014), ISSN 00219606, 1504.07652, URL `http://aip.scitation.org/doi/10.1063/1.4884276`.

[33] H. Hu, Z. Lu, and and Weitao Yang*, Journal of Chemical Theory and Computation **3**, 1004 (2007), ISSN 1549-9618, URL `http://dx.doi.org/10.1021/ct600295n`.

[34] C. C. I. Bayly, P. Cieplak, W. D. Cornell, and P. a. Kollman, The Journal of Physical ... **97**, 10269 (1993), ISSN 0022-

3654, 93/2091- 10269$04.00/0, URL http://pubs.acs.org/doi/abs/10.1021/j100142a004.

[35] U. C. Singh and P. A. Kollman, Journal of Computational Chemistry **5**, 129 (1984), ISSN 1096987X.

[36] P. G. Scherer and J. Seelig, Biochemistry **28**, 7720 (1989).

[37] O. H. S. Ollila and M. Retegan, *Md simulation trajectory and related files for popc bilayer (lipid14, gromacs 4.5)* (2014), URL http://dx.doi.org/10.5281/zenodo.12767.

[38] A. Botan, F. Favela-Rosales, P. F. J. Fuchs, M. Javanainen, M. Kanduč, W. Kulig, A. Lamberg, C. Loison, A. Lyubartsev, M. S. Miettinen, et al., J. Phys. Chem. B **119**, 15075 (2015).

[39] O. S. Ollila and G. Pabst, *Atomistic resolution structure and dynamics of lipid bilayers in simulations and experiments* (2016), in Press, URL http://dx.doi.org/10.1016/j.bbamem.2016.01.019.

[40] N. Kučerka, M. P. Nieh, and J. Katsaras, Biochim. Biophys. Acta **1808**, 2761 (2011), ISSN 0006-3002.

[41] T. M. Ferreira, R. Sood, R. Bärenwald, G. Carlström, D. Topgaard, K. Saalwächter, P. K. J. Kinnunen, and O. H. S. Ollila, Langmuir **32**, 6524 (2016).

[42] A. Seelig and J. Seelig, Biochemistry **16**, 45 (1977).

[43] J. H. Davis, Biochim. Biophys. Acta - Reviews on Biomembranes **737**, 117 (1983).

[44] G. Beschiaschvili and J. Seelig, Biochim. Biophys. Acta - Biomembranes **1061**, 78 (1991).

[45] D. K. Chattoraj and K. S. Birdi, *Adsorption at the Liquid Interface from the Multicomponent Solution* (Springer US, Boston, MA, 1984), pp. 83–131, ISBN 978-1-4615-8333-2, URL https://doi.org/10.1007/978-1-4615-8333-2_4.

[46] H. J. C. Berendsen, J. R. Grigera, and T. P. Straatsma, Journal of Physical Chemistry **91**, 6269 (1987), ISSN 0022-3654, URL http://links.isiglobalnet2.com/gateway/Gateway.cgi?GWVersion=2{\&}SrcAuth=mekentosj{\&}SrcApp=Papers{\&}DestLinkType=FullRecord{\&}DestApp=WOS{\&}KeyUT=A1987K994100038{\%}5Cnpapers2://publication/uuid/17978EF7-93C9-4CB5-89B3-086E5D2B9169{\%}5Cnhttp://pubs.acs.org/doi/pdf/10.1021/.

[47] S. Izadi, R. Anandakrishnan, and A. V. Onufriev, The Journal of Physical Chemistry Letters **5**, 3863 (2014), ISSN 1948-7185, 1408.1679, URL http://pubs.acs.org/doi/10.1021/jz501780a.

[48] S. Izadi and A. V. Onufriev, Journal of Chemical Physics **145**, 074501 (2016), ISSN 00219606, URL http://aip.scitation.org/doi/10.1063/1.4960175.

[49] W. L. Jorgensen, J. Chandrasekhar, J. D. Madura, R. W. Impey, and M. L. Klein, J. Chem. Phys **79** (1983).

[50] L. P. Wang, T. J. Martinez, and V. S. Pande, Journal of Physical Chemistry Letters **5**, 1885 (2014), ISSN 19487185, URL http://pubs.acs.org/doi/abs/10.1021/jz500737m.

[51] J. L. Abascal and C. Vega, The Journal of chemical physics **123**, 234505 (2005), ISSN 00219606, URL http://aip.scitation.org/doi/10.1063/1.2121687.

[52] D. E. Smith and L. X. Dang, J. Chem. Phys **100** (1994).

[53] T.-M. Chang and L. X. Dang, J. Phys. Chem. B **103**, 4714 (1999), ISSN 1520-6106, URL http://dx.doi.org/10.1021/jp982079o.

[54] L. X. Dang, G. K. Schenter, V.-A. Glezakou, and J. L. Fulton, J. Phys. Chem. B **110**, 23644 (2006), ISSN 1520-6106, URL http://dx.doi.org/10.1021/jp064661f.

[55] J. Åqvist, The Journal of Physical Chemistry **94**, 8021 (1990), URL http://dx.doi.org/10.1021/j100384a009.

[56] M. Girych and O. H. S. Ollila, *Popc_amber_lipid14_verlet* (2015), URL http://dx.doi.org/10.5281/zenodo.30898.

[57] M. Girych and O. H. S. Ollila, *Popc_amber_lipid14_cacl2_035mol* (2015), URL http://dx.doi.org/10.5281/zenodo.34415.

[58] M. Girych and S. Ollila, *Popc_amber_lipid14_cacl2_035mol* (2016), URL https://doi.org/10.5281/zenodo.46234.

[59] M. Girych and O. H. S. Ollila, *Popc_amber_lipid14_nacl_1mol* (2015), URL http://dx.doi.org/10.5281/zenodo.30865.

[60] M. J. Abraham, T. Murtola, R. Schulz, S. Páll, J. C. Smith, B. Hess, and E. Lindah, SoftwareX **1-2**, 19 (2015), ISSN 23527110, URL http://www.sciencedirect.com/science/article/pii/S2352711015000059.

[61] A. K. Malde, L. Zuo, M. Breeze, M. Stroet, D. Poger, P. C. Nair, C. Oostenbrink, and A. E. Mark, Journal of Chemical Theory and Computation **7**, 4026 (2011).

[62] D. Case, D. Cerutti, T. Cheatham, III, T. Darden, R. Duke, T. Giese, H. Gohlke, A. Goetz, D. Greene, et al., *AMBER 2017* (2017), university of California, San Francisco.

[63] A. W. SOUSA DA SILVA and W. F. VRANKEN, *ACPYPE - AnteChamber PYthon Parser interfacE.* (2017), manuscript submitted.

[64] O. H. S. Ollila, *POPC bilayer simulated at T313K with the Lipid14 model using Gromacs* (2017), URL https://doi.org/10.5281/zenodo.1020709.

[65] O. H. S. Ollila, *POPC bilayer with 10% of dihexadecyldimethylammonium simulated at T313K with the Lipid14 model using Gromacs* (2017), URL https://doi.org/10.5281/zenodo.1020240.

[66] O. H. S. Ollila, *POPC bilayer with 20% of dihexadecyldimethylammonium simulated at T313K with the Lipid14 model using Gromacs* (2017), URL https://doi.org/10.5281/zenodo.1020593.

[67] O. H. S. Ollila, *POPC bilayer with 30% of dihexadecyldimethylammonium simulated at T313K with the Lipid14 model using Gromacs* (2017), URL https://doi.org/10.5281/zenodo.1020623.

[68] O. H. S. Ollila, *POPC bilayer with 42% of dihexadecyldimethylammonium simulated at T313K with the Lipid14 model using Gromacs* (2017), URL https://doi.org/10.5281/zenodo.1020671.

[69] O. H. S. Ollila, *POPC bilayer with 50% of dihexadecyldimethylammonium simulated at T313K with the Lipid14 model using Gromacs* (2017), URL https://doi.org/10.5281/zenodo.1020689.

[70] T. M. Ferreira, F. Coreta-Gomes, O. H. S. Ollila, M. J. Moreno, W. L. C. Vaz, and D. Topgaard, Phys. Chem. Chem. Phys. **15**, 1976 (2013).

[71] A. Seelig and J. Seelig, Biochim. Biophys. Acta **406**, 1 (1975).

[72] H. Schindler and J. Seelig, Biochemistry **14**, 2283 (1975).

[73] K. Gawrisch, D. Ruston, J. Zimmerberg, V. Parsegian, R. Rand, and N. Fuller, Biophys. J. **61**, 1213 (1992).

[74] P. Auffinger, T. E. Cheatham, and A. C. Vaiana, Journal of Chemical Theory and Computation **3**, 1851 (2007), ISSN 1549-9618, URL http://www.researchgate.net/publication/228344458{_}Spontaneous{_}Formation{_}of{_}KCl{_}Aggregates{_}in{_}Biomolecular{_}Simulations{_}A{_}Force{_}Field{_}Issue.

[75] P. M. Macdonald and J. Seelig, Biochemistry **26**, 1231 (1987).
[76] D. Marsh, *Handbook of Lipid Bilayers, Second Edition* (RSC press, 2013).
[77] M. Javanainen, *POPC with varying amounts of cholesterol, 450 mM of CaCl_2. Charmm36 with ECC-scaled ions* (2017), URL https://doi.org/10.5281/zenodo.259376.
[78] D. Andelman, in *Handbook of biological physics* (Elsevier Science, 1995), vol. 1, chap. 12, pp. 603–642, URL http://hwiki.liebel-lab.org/wiki/images/9/90/AndelmannReview.pdf.
[79] G. Bussi, D. Donadio, and M. Parrinello, J. Chem. Phys **126** (2007).
[80] M. Parrinello and A. Rahman, J. Appl. Phys. **52**, 7182 (1981).
[81] T. Darden, D. York, and L. Pedersen, J. Chem. Phys **98** (1993).
[82] S. Páll and B. Hess, Computer Physics Communications **184**, 2641 (2013), ISSN 0010-4655, URL http://www.sciencedirect.com/science/article/pii/S0010465513001975.
[83] B. Hess, H. Bekker, H. J. C. Berendsen, and J. G. E. M. Fraaije, J. Comput. Chem. **18**, 1463 (1997).
[84] S. Miyamoto and P. A. Kollman, J. Comput. Chem **13**, 952 (1992).

ToDo

P.

1. We should also cite papers where empirical scaling was used ionic liquids DOI: 10.1002/anie.201308760 . 2
2. This needs a citation - Joe please pick 1-2 papers . . 2
3. To be uploaded to Zenodo 4
4. Provide the parameteres for ECC-surfactant somewere. 4
5. Dynamics check is missing: MSD (Hector/Joe) . . . 5
6. Add temperatures for POPC and DPPC experiments 6
8. Add OP-response of Lipid14+ECC-ions plot in SI . 6
7. Add temperatures to the experimental data. 7
9. Add columns with concentrations of calcium – bulk/molar fraction. 7
10. Changing symbol P to R or r might reflect better that it is rather a ratio, and not that much a probability. 7
11. JOE: I'll update this figure with some ensemble of configuration to support binding preference of Ca^{2+} SAMULI: I am not sure if this would be needed anymore. 8
12. Samuli: I think that we either have to do the analysis in SI properly, i.e., using the real C_I from simulations or remove the sentence below and the related concent from SI. Joe: I think it shows that ternary complex makes a good fit to our simulation data. The fact that we use a different (and more accurate) estimate of C_I and other quantities does not hamper this statement. 9
13. Add acknowledgments of Jiri Kolafa. 10
14. Joe: Thank Metacentrum. 10
15. This should be either done properly with the correct C_I or removed. Removing might be a better idea at this point. 11

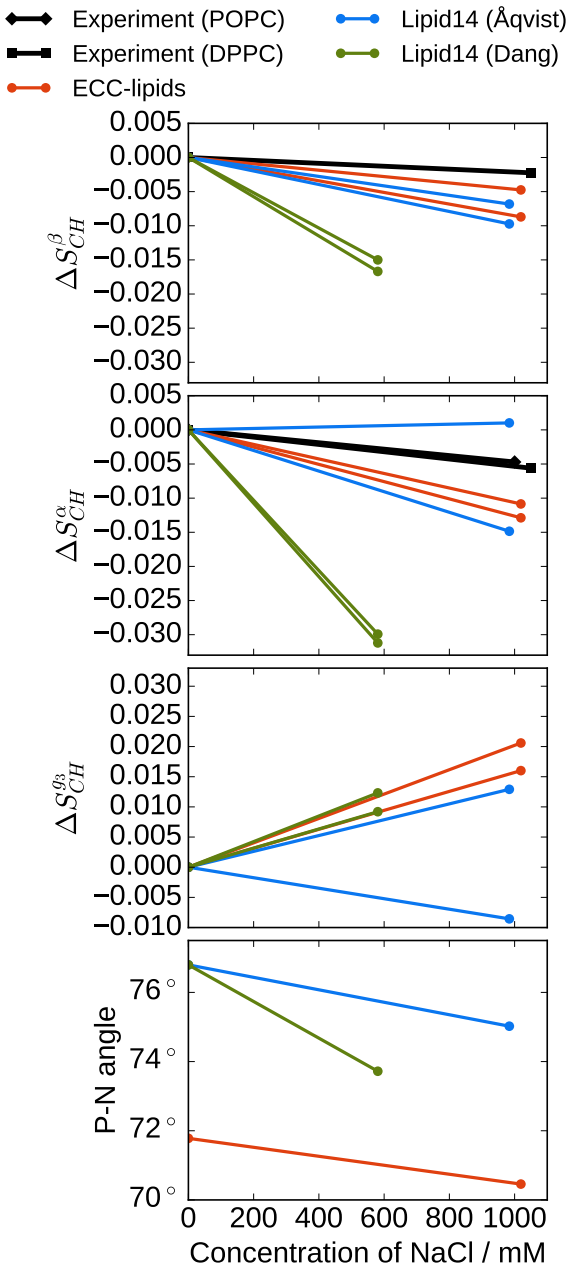

FIG. 10: Changes of head group order parameters of POPC bilayer as a function of NaCl concentrations are shown from simulations with different force fields together with experimental data [4]. Ion concentrations in bulk water are shown in x-axis. Values from simulations are calculated from the of cation number density C_{np} from the region at the simulatin box edge with the constant ion concentration as [ion]=$C_{np}/0.602$. Simulation data with Lipid14 and Åqvist ion parameters is taken directly from Ref. [18].

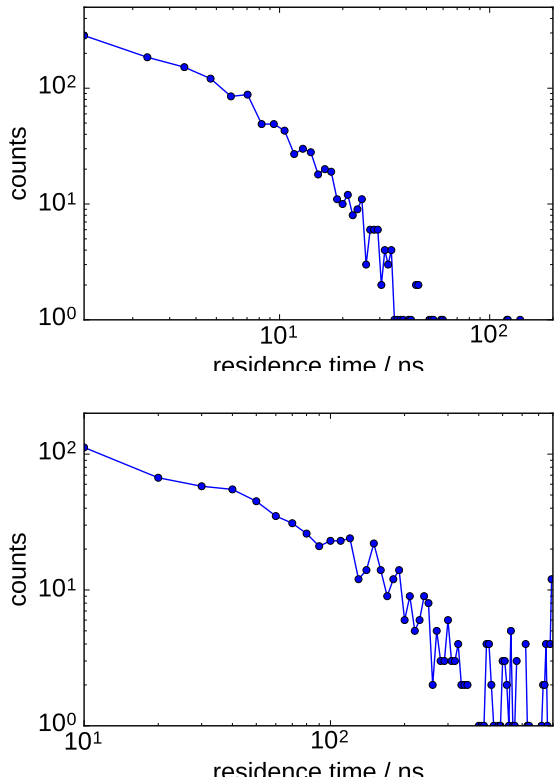

FIG. 11: Histograms of residence times of Ca^{2+} in a POPC bilayer at $450\,\mathrm{mM}$ concentration of $CaCl_2$ in water before adsorption to phospholipids from simulations with ECC-lipids/ECC-ions (top) and CHARMM36/ECC-ions (bottom), which was taken from previous study [14] (simulation data available at Ref. 77). The maxima on the x-axis represent the lengths of the simulations used for analysis. For the ECC-lipids model, 90% of the residence times of Ca^{2+} in a POPC membrane are shorter than $60\,\mathrm{ns}$, with the longest observed residence time being $141\,\mathrm{ns}$, which is well below the total length of the simulation (200 ns). This is, however not true for the simulation with CHARMM36 model, where there are several calcium cations with their residence time apparently limited by the length of the simulation. With such a simulation, which is relatively short for the employed model, we can merely estimate an upper bound that only less than 60% of the bound residence time is formed by cations interacting with the phospholipid membrane for less then half of the simulation length (400 ns).